*33rd EPS Conference on Plasma Phys. Rome, 19 - 23 June 2006 ECA Vol.**30I**, O-2.008 (2006)*

Ultrafast Laser Driven Micro-Lens to Focus and Energy Select MeV Protons

Toma Toncian[1], Marco Borghesi[2], Julien Fuchs[3], Emmanuel d'Humières[3,4], Patrizio Antici[3], Patrick Audebert[3], Erik Brambrink[3], Carlo Alberto Cecchetti[2], Ariane Pipahl[1], Lorenzo Romagnani[2], Oswald Willi[1]

[1] *Heinrich Heine Universität Düsseldorf, Düsseldorf, Germany*

[2] *School of Mathematics and Physics, The Queen's University Belfast,Belfast, United Kingdom*

[3] *Laboratoire pour l'Utilisation des Lasers Intenses, Palaiseau, France*

[4] *Centre de Physique Théorique, Palaiseau, France.*

The acceleration of MeV ions from the interaction of high-intensity laser-pulses with thin solids has major applicative prospects due to the high beam quality of these ion bursts ([1],[2]). However, as these proton beams are poly-energetic and divergent at the source, reduction and control of their divergence and energy spread are essential requirements for most of these applications. We have developed a device which provides tuneable, simultaneous focusing and energy selection of MeV proton beams ([3]). Compared to techniques ([4],[5]) employing complex target fabrication or preparation procedures, our method decouples the beam tailoring stage from the acceleration stage allowing for their independent optimization. The method employs a compact laser driven micro-lens arrangement, a schematic of which is shown in Fig 1A. Figs 1B-C sketch the underlying physical process: relativistic electrons injected through the cylinder's wall by the CPA_2 laser pulse spread evenly on the cylinder's inner walls and initiate hot plasma expansion. The transient electric fields associated with the expansion are employed, in a radial geometry, to focus protons accelerated by the CPA_1 laser pulse from a thin planar foil. The micro-lens operation was demonstrated in experiments carried out at the LULI Laboratory, em-

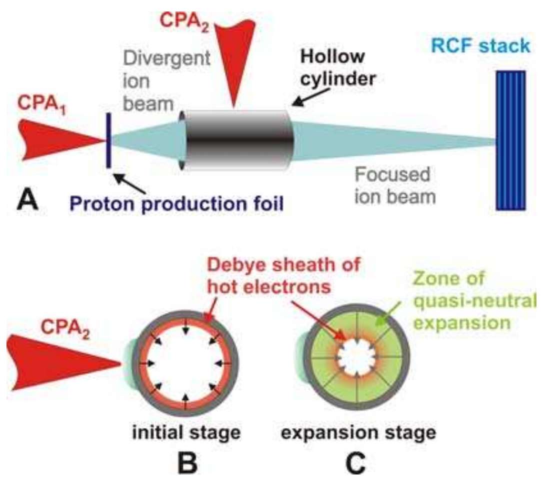

Figure 1: (A) Schematic of the micro-lens device. A proton beam is accelerated from a planar foil by the CPA_1 laser pulse propagates through a hollow cylinder side-irradiated by the CPA_2 laser pulse. (B,C) Schematic of the operation's principle of the micro-lens. The CPA_2 laser pulse injects hot electrons within the cylinder. These electrons generate a space-charge field (indicated by the radially pointing arrows), which then induces plasma expansion (C) from the cylinder's inner walls.

ploying the 100 TW laser ([6]) operating in the Chirped Pulse Amplification mode (CPA). After amplification, the laser pulse was split into two separate pulses (CPA_1 and CPA_2) which were recompressed in separate grating compressors to a 350 fs duration.

The delay between the two pulses was controlled optically with picosecond precision. The CPA_1 pulse (irradiance $I=5\times10^{19}$ W/cm^2) was used to accelerate a high-current, diverging beam of up to 15 MeV protons from a 25 μm thick Al foil target (the protons are produced from hydrocarbon impurities ([7]) on the target rear surface ([9],[10])). The CPA_2 pulse ($I = 3\times10^{18}$ W/cm^2) was focused onto the outer wall of a hollow cylinder.

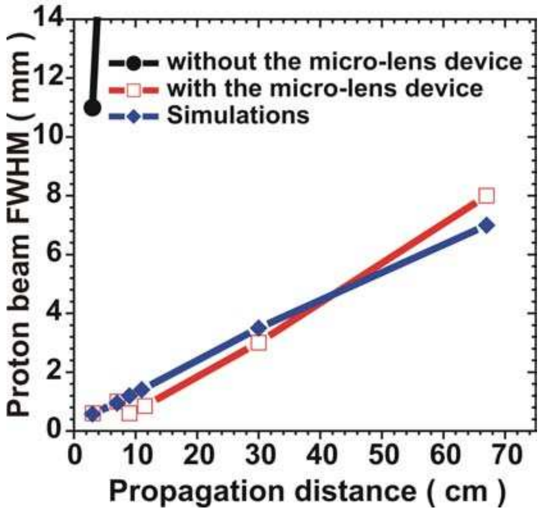

Figure 2: Evolution of the FWHM of the proton beam, for protons with an energy of 7.5 MeV (The propagation distance is calculated from the proton source). The black circles correspond to the case without micro-lens (free-space divergence), the blue diamonds to the particle-tracer simulation in the fields given by the PIC simulation, and the red squares to the experimental results using the micro-lens.

The proton beam from the first foil was directed through the cylinder and detected with a stack of Gafchromic Radiochromic Films (RCF, a dosimetric detector positioned at a variable (from 2 to 70 cm) distance from the proton source. An RCF pack was recording the proton beam after its propagation through a laser-illuminated dural cylinder 3 mm in length, 700 μm in diameter and 50 μm in wall thickness. The entrance plane of the cylinder was placed 4 mm from the proton producing foil. The distance from the proton-producing foil to CPA_2 irradiation point on the cylinder was 5 mm. Focal spots as small as 200 μm have been observed depending on the detector position. In this case the proton flux within the spot at the film plane is increased by up to 15 times compared to the unfocused part not captured by the cylinder. We have studied the evolution of the beam size, as a function of the propagation distance from the cylinder.The behaviour of the 7.5 MeV proton component, is illustrated in Figure 2. Note that for this energy, the beam size is only 8 mm after 70 cm of propagation whereas freely propagating, the size of the beam would have been ~ 260 mm.

1D and 2D Particle-in-Cell simulations using the CALDER code ([8]) of field generation at the micro-lens' walls and 3D test-particle simulations of proton propagation through the micro-lens were performed. The results support the above mentioned scenario in which laser-triggered transient fields drive the selective deflection of the protons. The physical mechanisms behind the micro-lens operation are as follows: when the laser pulse irradiates the outer side of the cylinder, it produces a population of hot electrons which penetrate through the wall and spread very quickly over the inner surface of the cylinder. They then exit into vacuum resulting in an electron cloud in the surface surrounding area. The associated space-charge field is large enough to ionize the material at the cylinder surface and to create plasma. This results in a cylindrical plasma layer with high electron temperature T_e . The plasma begins to expand towards the cylinder axis, driven by a hot electron sheath that extends over a Debye length ahead of the plasma ([9],[10],[11]).

The radially symmetric ambipolar electrostatic field associated with the plasma front is responsible for the variable focusing of the protons propagating along the cylinder's axis. The poly-energetic protons arrive in the cylinder at different times due to their different velocities, with higher energy protons crossing the cylinder at earlier times. Protons passing through the micro-lens before it is triggered, do not experience any fields and are therefore not deflected. Protons which are crossing the cylinder and are close to its end when it is triggered and therefore experience the fields for only a short time will be collimated. Lower energy protons will experience a larger cumulated field along their propagation through the cylinder. They are therefore focused at a short distance from the exit plane of the micro-lens and diverge strongly after focus. This results in a diluted beam on the RCF stack positioned a few cm away and in the strong dip observed in the spectrum of Figure (3) in below 6 MeV.

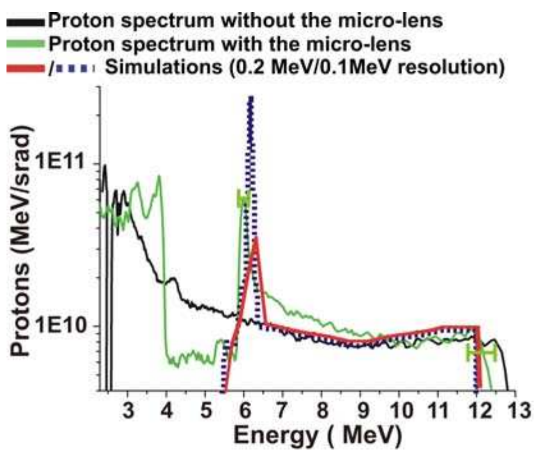

Figure 3: Experimental proton spectra measured in the experiments using a magnetic spectrometer without micro-lens (black line) and with the microlens (green line), and proton spectrum simulated using a simulation code (red and dotted lines) performed with the user of the experimental proton beam parameters (i.e. the spectrum without micro-lens) and magnetic spectrometer parameters (i.e. distance from the source and slit characteristics). The simulated spectrum was obtained by tracing 5000 protons for each energy considered through the fields predicted by the PIC simulation.

Additional simulations were performed to test the scalability of the micro-lens to higher proton energies, as needed for applications such as proton therapy. We compute that, using the same cylinder as in our experiment and a slightly more intense CPA_2 triggering laser pulse (10^{19} W/cm^2), we can induce collimation of 270 MeV protons. Protons of such high energy transit through the micro-lens in a short time (13 ps), therefore a higher intensity in the order of 10^{20} W/cm^2 is required to focus strongly protons of such energies. We note that simulations predict mono-energetic protons in the GeV range at intensities of 10^{23} W/cm^2 ([12]). In this case, the micro-lens could still prove to be useful to provide beam focusing. The focusing device described has potential use in all applications of energetic protons in which a large flux of protons or a narrow spectral beam are required. These include most of the proposed applications in the medical and technological areas. For example, focusing ion beams opens new perspectives to further developments in areas such as hadron therapy for cancer treatment, accelerator physics and inertial fusion physics. Besides applications using laser-driven ion beams, such a device might find application as focusing/fast switching tools for ion beams produced from conventional accelerators.

References

[1] M. Borghesi et al., Phys. Rev. Lett. **92**, 055003/1 (2004).

[2] T. Cowan et al., Phys. Rev. Lett. **92**, 204801/1 (2004).

[3] T. Toncian et. al., Science **312**, 410 (2006)

[4] B.M. Heglich et al., Nature **439**, 441 (2006)

[5] H. Schwoerer et al., Nature **439**, 445 (2006).

[6] B. Wattellier et al., Opt. Lett. **29**, 2494 (2004).

[7] M. Hegelich et al., Phys. Rev. Lett. **89**, 085002/1 (2002).

[8] E. Lefebvre et al., Nucl. Fusion **43**, 629 (2003).

[9] S.C. Wilks et al., Phys. Plasmas **8**, 542 (2001).

[10] L. Romagnani et. al., Phys. Rev. Lett. **95**, 195001/1 (2005).

[11] S. Gordienko, T. Baeva and A. Pukhov, arXiv.org:physics/0511070.

[12] T. Esirkepov, M. Borghesi, S.V. Bulanov, G. Mourou and T. Tajima, Phys. Rev. Lett. **92**, 175003 (2004)